

# COMPARISON BETWEEN THE RESULTS OF IMPLEMENTATION OF SENSORLESS SLIDING MODE CONTROL USING SLIDING MODE OBSERVER AND SENSORLESS SLIDING MODE CONTROL USING MRAS-HG OBSERVER OF AN INDUCTION MOTOR ON AN FPGA BOARD

<sup>1</sup>SGHAIER NARJESS, <sup>2</sup>BEN AMMAR IMEN, <sup>1</sup>MIMOUNI MED FAOUZI

<sup>1</sup> The National Engineering School of Monastir, Ibn El jazzar City, 5019, Monastir,

<sup>2</sup> The Higher Institute of Technological Study of Kelibia, Oued el Khatef City, 8090, Kelibia,

E-mail: <sup>1</sup>sghaier\_narjess@yahoo.fr, <sup>2</sup>benammarimen81@yahoo.fr, <sup>1</sup>Mfaouzi.mimouni@enim.rnu.tn

## ABSTRACT

In this paper we will focus on the results of the implementation on an experimental test bench of an Induction motor using the FPGA Board of two types of sensorless sliding mode control. A comparison will be made between the results obtained from the sensorless sliding mode control based on the one part on a sliding mode observer and on the other part on a MRAS-HG observer.

**Keywords:** *Induction Motor, FPGA, Sensorless Control, Sliding Mode observer, MRAS-HG observer, experimental test bench*

## 1. INTRODUCTION

To control a three-phase asynchronous machine, we must have a perfect knowledge of its state. Also, it is necessary to access for all its magnitudes of state. For this, we need several mechanical and electrical sensors. Unfortunately, its sensors have several disadvantages: they are very expensive because of the measurement accuracy; they are very sensitive to external disturbances. Not to mention that the cost of maintenance of the sensors is very high and they add additional wiring between the machine and the drive. And the major problem that some variables are not accessible to the extent. The adequate solution to this problem is the use of sensorless control. The problem with this type of control is the reconstitution of non-measurable information which is the rotor flux and the speed in the case of the sensorless control. The first solution is the use of a state estimator. The second is the use of a state observer. In this article we will use two types of observer: the sliding mode observer and the MRAS observer associated to a High Gain observer (MRAS-HG).

Two questions that are necessary here the first: can we implement experimentally this solution

proposed to remedy the previous problems? And second, what is the contribution of this paper compared to the research done previously?

The contribution of this paper is the comparison of the results of the experimental implementation of two types of sensorless sliding mode control of an induction motor. The first is based on a sliding mode observer and the second one is based on an MRAS-HG observer. The experimental implementation is done on a test bench based on an FPGA board using a new tool named Xilinx System Generator (XSG).

## 2. PRESENTATION OF THE EXPERIMENTAL TEST BENCH

### 2.1 Validation of the control architecture

In order to validate the designed architecture, we must use XSG tool associated with MATLAB-SIMULINK. Using this step we can verify the realized architecture using a hardware language of description. This architecture after it is validated can be immediately implemented on FPGA then this FPGA card is connected to the experimental test bench. Not to mention that the majority of designers try to push the verification of the results of the command using the tool "Hardware in the

loop". This type of verification is divided into two major parts:

- The first part aims to generate "Stimulus". These are the inputs of the control algorithm.
- The second part is the algorithm to check.

## 2.2 Experimental test bench

The experimental test bench validates the results obtained by simulation performed using the

MATLAB-SIMULINK tool. This bench consists of four main parts:

- The Power part
- The Control part
- An acquisition and measurement interface
- A man / machine interface for the control of the inverter



Figure 1: Pictures of the experimental test bench

### 2.2.1 The power part

The power section of this test bench comprises:

- **Asynchronous machine:** the electrical machine of the test bench is a LEROY SOMER brand squirrel cage three-phase induction machine with a rated power of 1.5KW. The machine is equipped with forced ventilation and an incremental position sensor of 1024 points.
- **Mechanical load:** this is a load associated with the asynchronous machine. It consists of an electromagnetic powder brake brand

LEROYSOMER. It is mechanically coupled to the motor shaft and develops a constant and adjustable resistive torque according to its excitation current in both directions of rotation of the motor. This brake is thermally protected at a temperature threshold above 85 °C.

- **Controlled converter:** the converter is of SEMIKRON type. The converter consists of:
  - *a three-phase rectifier:* its role is to transform a three-phase AC voltage into a DC voltage of well-determined average value depending on the nature of the

rectification and the RMS value of the AC voltage at the input of the rectifier. The supply voltage of the rectifier is three-phase 380V and its output is a DC voltage of up to 537V.

- *a three-phase voltage inverter*: its role is to deliver from a DC voltage an AC voltage of variable amplitude and frequency. The synoptic of our inverter contains three arms. Each of these arms contains two "SIEMENS" IGBT power switches. The calculation of the switching frequency of the inverter shows the opening time, the closing time and the dead time of the switches of the same arm. The maximum switching frequency of this inverter is 20KHz. The rated current of the inverter is set at 50A and the nominal apparent power is of the order of 20KVA.
- **Electrical source**: We have a three-phase network (380V / 50Hz) and a three-phase

autotransformer. The role of the autotransformer is to generate a three-phase voltage source of adjustable amplitude.

### 2.2.2 The Control part

The FPGA type control card used is of the Virtex5 type, reference ML507 XC5VFX70T from Xilinx. We opted to choose this map given the number of resources it has. Indeed, it is composed of 11200 slices and it has RAM memory blocks of global size 5328Kb. The specificity of this card is that it has a clock frequency of 100MHz. It has several input and output ports of high logic level 3.3V. Also, it contains communication ports with RS232 and USB external elements. This card also contains 128 DSP48E modules each of these modules contains: a subtractor, a multiplier, an adder ... Indeed, the role of this card is the implementation of the different control algorithms.

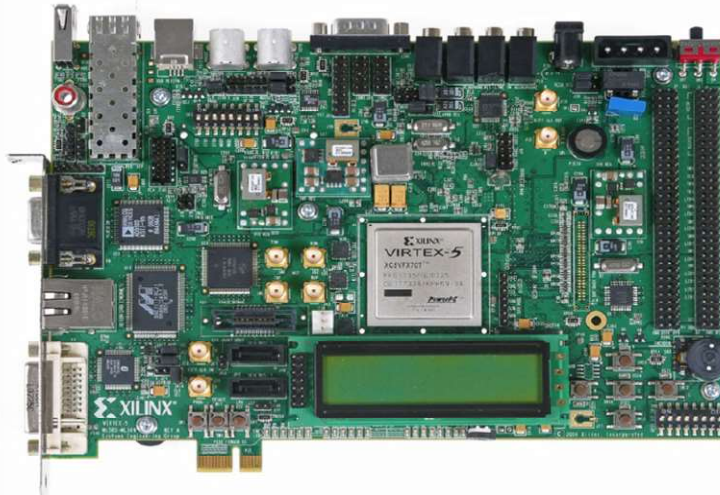


Figure 2: The Virtex 5 control board made of FPGA

- **Encoder interface IC**: The incremental encoder mounted on the shaft of the asynchronous machine is used to give the rotor speed. The incremental encoder we have in our experimental test bed has 1024 slits. The latter gives as output three signals  $U_1$  and  $U_2$  which have a phase shift of  $90^\circ$  and  $U_{10}$  which generates a pulse for each mechanical revolution. Indeed, the phase quadrature between  $U_1$  and  $U_2$  determines the direction of rotation.
- **The Control**: Whatever the type of the control, this block always receives as input signal the currents  $i_A$  and  $i_B$  which come from the current sensors and which then pass through the analog/digital conversion board. And the output signals of this module are always the control signals of the inverter  $S_a$ ,  $S_b$  and  $S_c$ .
- **Human / machine interface for the control of the inverter**: the role of this interface is to ensure communication between the manipulator and the controlled system. To do this, a host computer allows in one direction to send the reference instructions to the FPGA card and in another to acquire the variables processed in the control algorithm. This interface was developed under Visual Basic, reads data from the serial port. This interface

allows the graphic visualization of the received data as well as the backup on the hard disk for an interior use.

- **DAC interface:** It is an interface that serves to control the analog / digital conversion. This interface allows the acquisition of analog values of currents and voltages and to convert them into numerical values. At each rising edge of the clock, digital data in binary format is accessible. This interface controls through a data read clock the sending of a conversion start signal and the reception of an end of conversion signal. Our converter is of type ADS8509 with a resolution of 16bits.
- **Serial communication interface:** Through the existing RS232 port in the FPGA card it is possible to exchange data between the computer and the FPGA card. Indeed, this interface allows the exchange of information in both directions of the computer to the FPGA card and vice versa.

### 2.2.3 An acquisition and measurement interface:

Whatever the type of control applied to the asynchronous machine we must always perform the acquisition of the electrical variables of our machine. The acquisition of two currents for example  $i_A$  and  $i_B$  is largely sufficient to carry out the control because we have a balanced three-phase system; the third current is calculated as follows:  $i_C = -(i_A + i_B)$ . Indeed, the role of the measurement and acquisition interface is to obtain the values of the two currents then transmit them to the control part in digital form. Our measurement and acquisition interface comprises several modules. The first module of this interface is the current sensor. This sensor enables the acquisition of the two stator currents. The selected current sensors are LEM: LA25-NP type hall effect

sensors. We have chosen to choose this type of sensor given the advantages they have: a good accuracy a very low sensitivity to external disturbances, a very easy implementation ... This sensor is always associated with conditioner that can convert the output of the sensor in a voltage. Then this signal is amplified using the operational amplifiers. The fourth module of this acquisition and measurement interface is the analog filter. In fact, this filter is a quadripole that allows the filtering of a signal by transmitting only the frequency band. The last element of this acquisition and measurement interface is an analog digital converter whose role is to convert currents from the acquisition card to digital greatness . The digital analog conversion is provided by an ADS8509 converter characterized by a resolution of 16 bits series and a conversion time of  $2.2\mu s$  and a multiplexer whose purpose is to choose a stator current among the two. The operation of this converter requires the generation of the control signals. To generate these signals we used the XSG environment

### 2.2.4 Inverter control interface:

The control interface of the inverter must first allow isolation between the power signals (inverter control) and the control signals generated by the FPGA. Then these signals must be amplified. Because the signals coming from the FPGA card are of level 3.3 V whereas the control signals of the switches of the inverter must be of 15V. For the three control signals of the inverter  $S_a$ ,  $S_b$ ,  $S_c$ , fixed dead times will be created for the commands  $S'a$ ,  $S'b$ ,  $S'c$ . The goal of creating these downtime is to avoid short circuits between the closing and opening of the same inverter arm. Finally, the control interface of the inverter must allow the optical isolation of the inverter and the close control board.

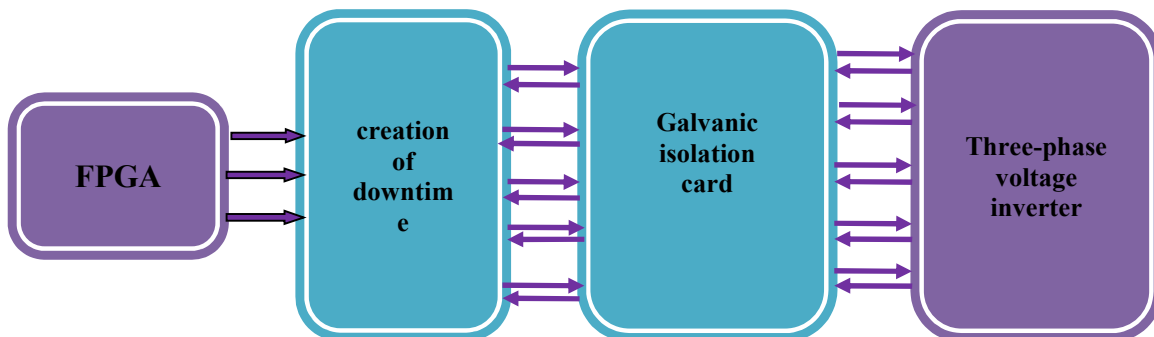


Figure 3: Synoptic diagram of the close control card

The realization of this control interface of the inverter must go through the realization of two cards. The first card is a downtime creation card and the second card is the isolation and amplification card of the control signals.

**a- Downtime creation card**

Actually, all IGBT transistors have a delay time on closing and a time delay on opening. In order to avoid the risks of conduction of two switches of the same inverter arm and to avoid short circuits, it is necessary to delay the conduction of the two switches of the same arm by the insertion of a dead time between a signal of control of an inverter and its complementary. Just, it must be ensured that this timeout must be greater than the delay time at closing and opening of the IGBT. The time-out creation card makes it possible to generate from a signal two signals shifted by a dead time of 3  $\mu$ s.

**b- Amplification and isolation card for control signals**

This board allows amplification of 3.3V signals at the FPGA up to 15V at the input of the inverter.

Apart from the amplification of the control signals of the inverter, we must guarantee the galvanic isolation between the control board of the FPGA and the close control board of the inverter. For amplification and isolation, optocouplers type 6N136 are used. So the logic signals from the FPGA board connect to the input of optocouplers, the latter are powered by a voltage of 15V.

Our SEMIKRON inverter consists of a protection system. This system can generate a signal in the event of a fault (overcurrent, overvoltage, short circuit or an increase in temperature). These signals have been exploited in the realization of the galvanic isolation board and amplification of the signals to be able to render inactive the control signals as soon as a defect is detected. The figure below is a block diagram of the experimental test bench where there are the different parts detailed previously.

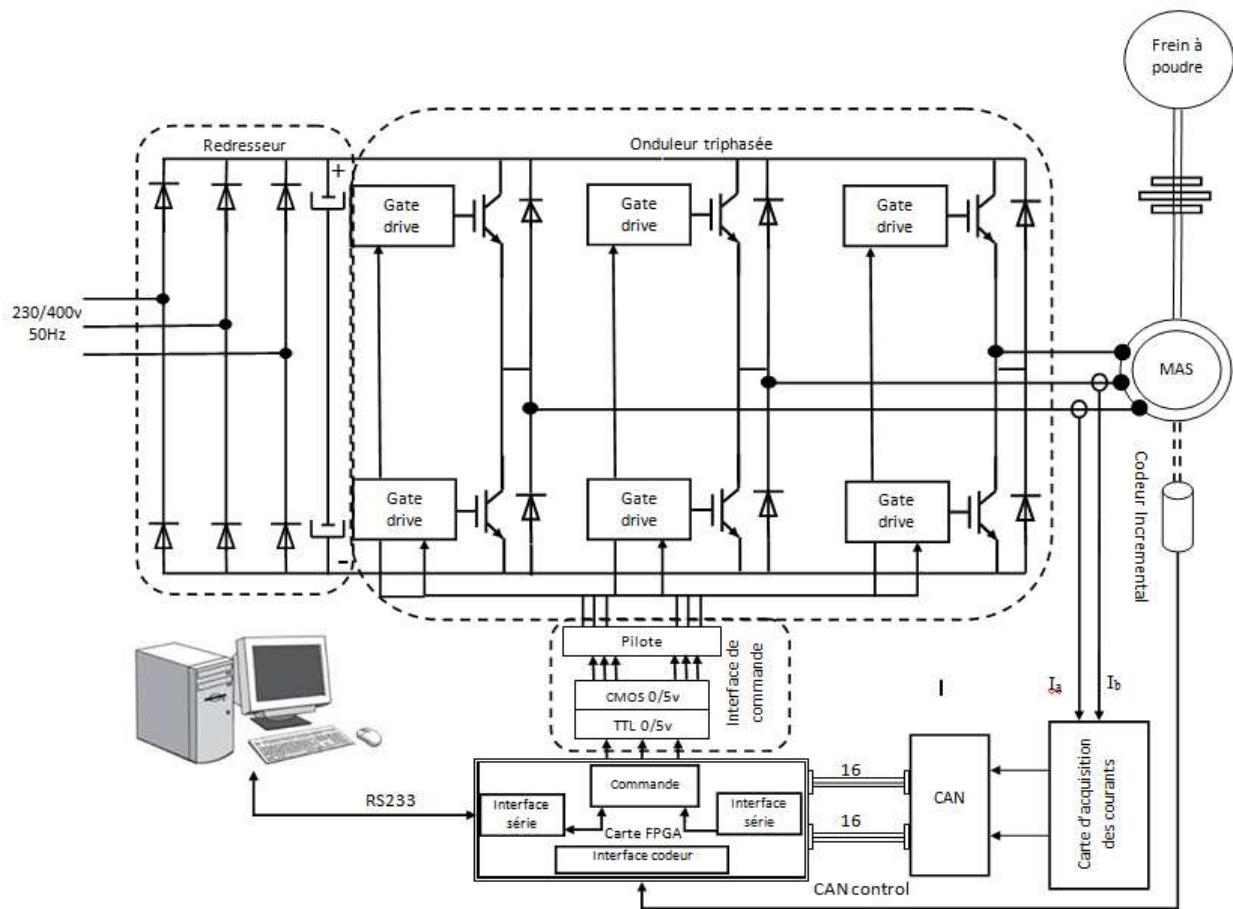


Figure 4: Synoptic diagram of the experimental test bench

### 3. IMPLEMENTATION OF SENSORLESS SLIDING MODE CONTROL BASED ON SLIDING MODE OBSERVER ON FPGA BOARD

In order to highlight the performances of the sliding mode observer applied to the sliding mode control without mechanical sensors. Below you will find the explanatory diagram containing the different blocks.

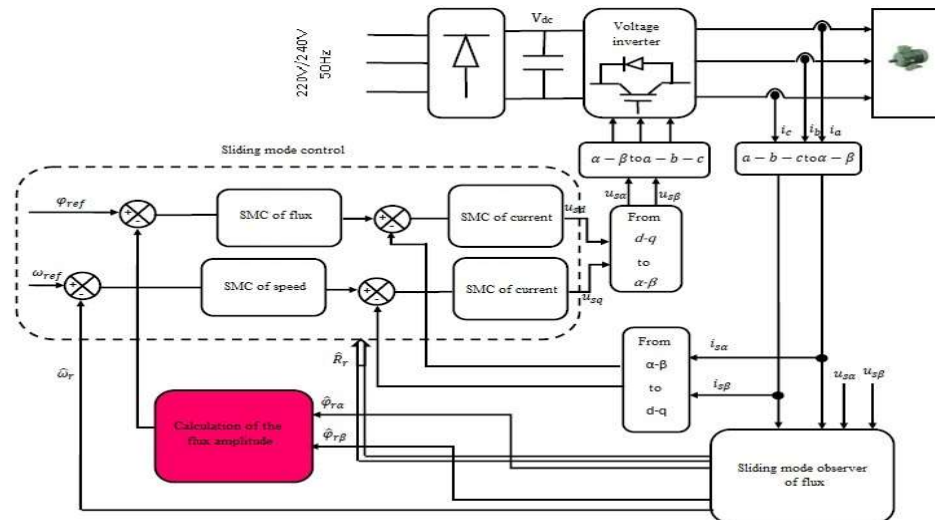


Figure 5: Block diagram of a Sliding Mode control with a sliding mode observer

#### 3.1 Desing of sliding mode observer using xilinx system generator

XSG is a tool box developed by Xilinx to be integrated into the MATLAB-Simulink environment and allows users to create highly parallel systems for FPGAs. The models created are displayed as blocks and can be linked to other blocks and all other boxes MATLAB-Simulink tools. Once the system is completed, the VHDL code generated by the XSG tool replicates exactly the behavior observed in MATLAB. It is much easier to analyze the results with MATLAB than

the other tools like ModelSim associated to VHDL. Then, the model may be coupled to virtual engines. The XSG tool is used to produce a model that will immediately work on equipment when completed and validated. In this part we will remake the control algorithms performed using MATLAB-Simulink using the XSG tool. So we designed all sub blocks of the sliding mode observer of the flux and the stator currents. We will collect them, connect them and realize the overall scheme of our observer realized in the XSG environment is shown in figure 6.

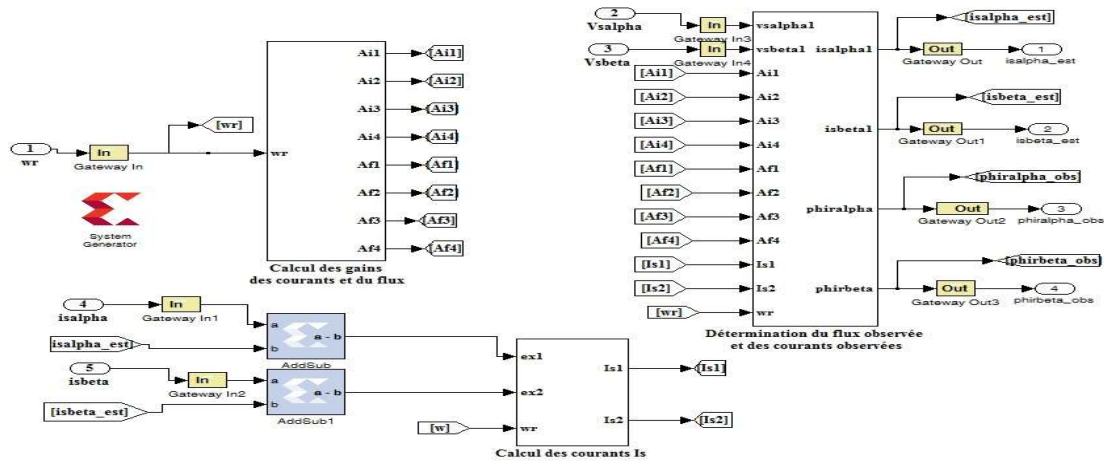


Figure 6: Overall scheme of the block of the sliding mode observer designed with the tool XSG

**3.2 Results:**

In this part we will present the results as a comparison between the results found using MATLAB-SIMULINK (simulation) and XSG (real implementation).

For the speed setpoint, we start with the magnetization regime of the machine, then we apply a ramp of speed at  $t = 0.1s$  to reach its reference value (100 rad / s) at  $t = 0.3s$ . Then, at  $t = 1.2s$  we apply a negative speed to the machine reaching a value of (-50 rad / s) at  $t = 1.2s$ . The nominal value of the reference flux is equal to 0.9 Wb.

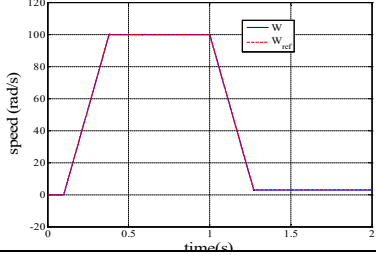
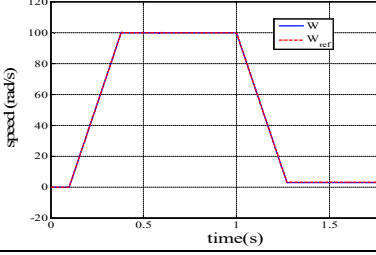
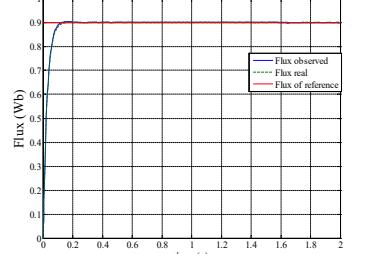
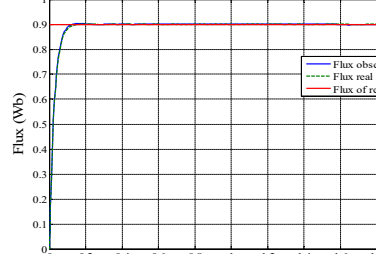
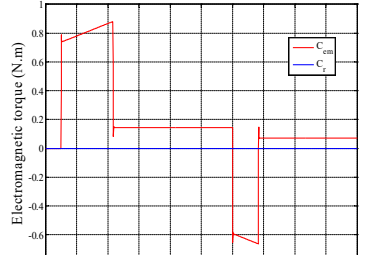
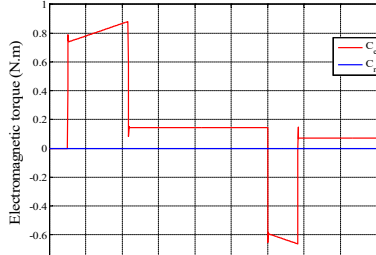
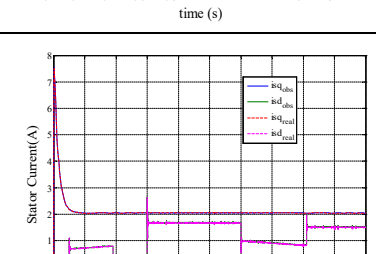
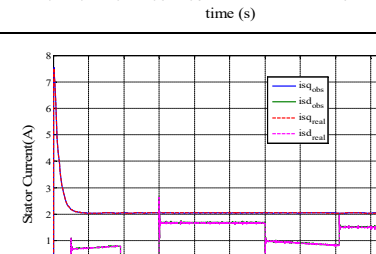
According to these results obtained by performing these tests, we can conclude that the sliding mode control with the sliding mode observer gives very satisfactory results. This sensorless control demonstrated a good robustness against parametric variations. This type of control has displayed a perfect decoupling between flux

and torque. And the most important that the results obtained with the XSG environment are similar to those obtained with SIMULINK. Also, we found flawless results with XSG during the actual implementation.

**4. IMPLEMENTATION OF SENSORLESS SLIDING MODE CONTROL BASED ON MRAS-HG OBSERVER ON FPGA BOARD**

As illustrated in the diagram below, we will begin by associating MRAS-HG observer to the Sliding Mode Control. This type of command allow to ensure complete system stability. But unfortunately it is very sensitive with respect to the variation of the rotor time constant. That is why it is necessary, as shown in the diagram, to highlight an adaptive mechanism of the rotor resistance online because it greatly affects the efficiency of MAS. Also to highlight the importance of the latter, several types of tests will be performed thereafter.

Table 1: Results of the sensorless sliding mode control with a sliding mode observer

Sensorless sliding mode control with sliding mode observer		
	MATLAB-SIMULINK	XSG
Speed (rad/s)		
Flux (Wb)		
Electromagnetic torque (N.m)		
Stator Current $i_{sd}, i_{sq}$ (A)		



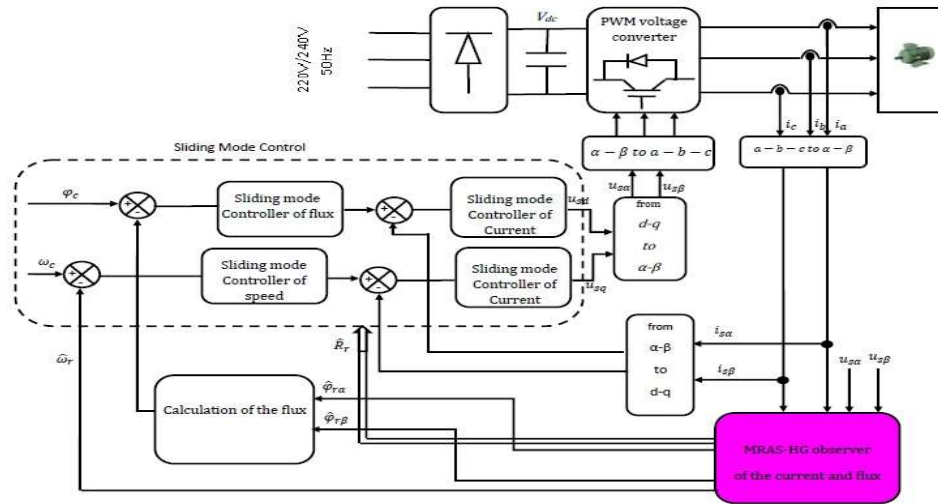


Figure 7: Block Diagram of Sliding mode control with MRAS-HG observer

#### 4.1 Results:

To test the performance and robustness of the Sliding control without mechanical sensor with MRAS-HG observer in different areas of operation. We do a series of tests concerning on the change of different variables of machine: (speed, load).

- **Test: speed variation and the application of the load torque**

For the speed setpoint, we start with the magnetization regime of the machine, then we apply one speed ramp at  $t = 0.1s$  to reach its reference value (100 rad / s) at  $t = 0.3s$ . Then, at  $t = 1.2s$  we apply a speed reverse of the machine to a value of (-50 rad / s) at  $t = 1.2s$ . The nominal value of the reference flux is equal to 0.9 Wb. We apply a value of load torque 4 N.m at  $t = 0.6s$ . Simulation results obtained with this first test are illustrated in the table below:

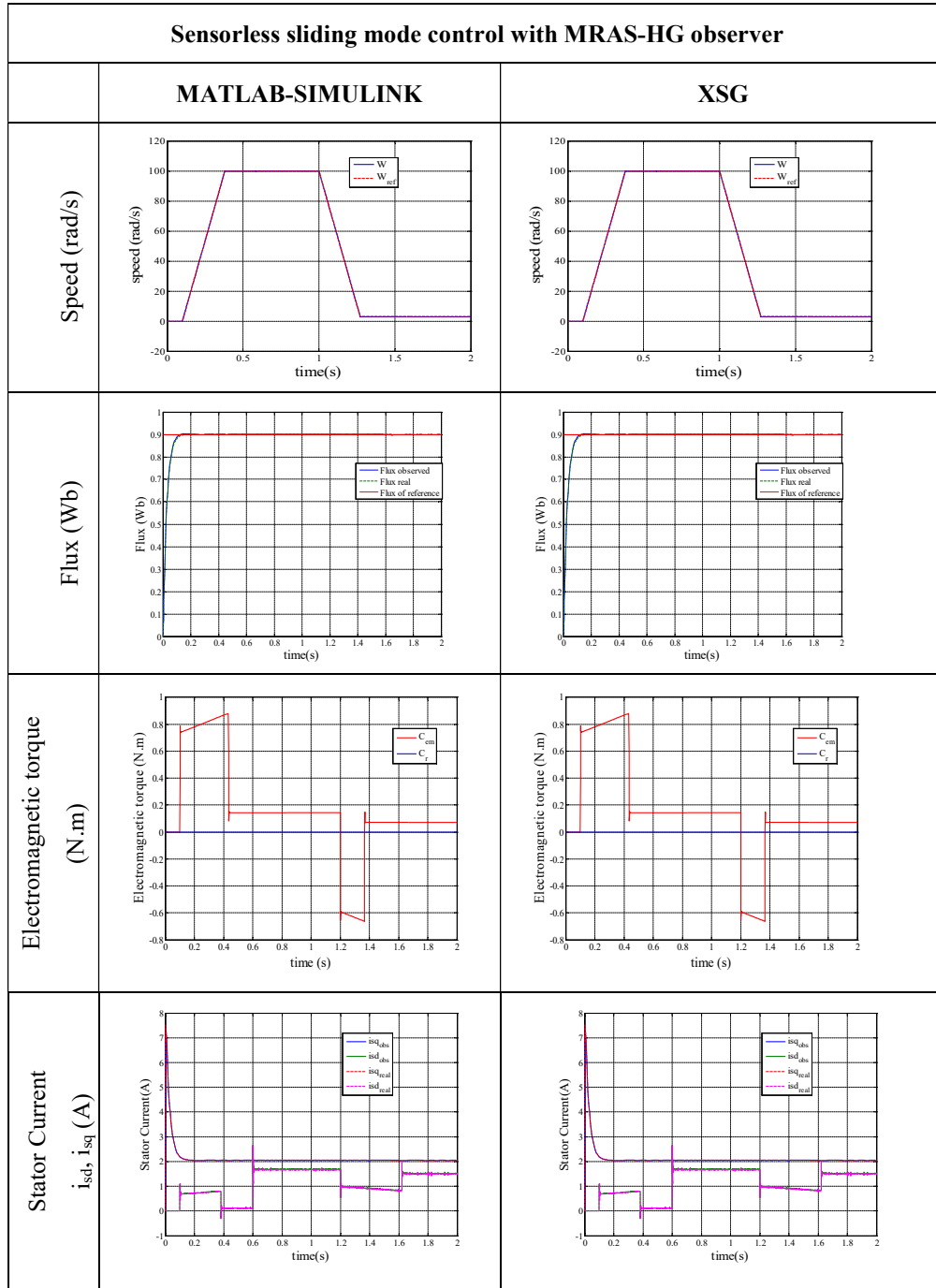


Table 2: Results of sensorless sliding mode control with MRAS-HG observer

From these results, we note that the speed and the flux perfectly follow their reference values in all areas of operation which involves that the robustness of this control vis a vis of the speed variation.

After we apply of a load torque at  $t = 0.6s$ , analyzing the behavior of our MRAS observer based on an observation of the stream by a high gain observer shows a perfect decoupling between

the flux and the rotor speed. Indeed, this variation does not affect the rotor flux.

From these results obtained by performing these tests, it can be concluded that the sliding mode control associated with the MRAS observer gives very good results. In fact, this command is very robust with respect to parametric variations. Thanks to this command, decoupling is ensured between the flow and the torque. These results are identical to those obtained with the sliding mode observer. The results obtained with XSG and SIMULINK are perfectly similar.

This is the first time compared to previous research work that we carry out an experimental implementation of a sensorless control of a three-phase asynchronous machine using two different types of observers on an experimental test bench based FPGA. In addition the experimental results found are similar to the simulation results which reflects the effectiveness of this chosen method.

## 5. CONCLUSION

In this paper we used two deterministic, nonlinear observation approaches applied to the asynchronous machine. The first observer is the sliding mode observer and the second observer is the MRAS observer combined with the large gain observer. Then we applied these observers to the sliding mode command. We designed sensorless controls with XSG for FPGA implementation. At the end, a comparative study was made between the results obtained by the two observers with XSG and SIMULINK and it can be concluded that we obtained impeccable experimental results. In addition, by performing several tests it can be concluded that these two approaches (sliding mode observers, MRAS observer combined with the High Gain observer) will satisfy the most critical requirements of MAS control laws from robustness point of view and parametric variations and they will ensure proper operation over the entire speed range especially during low speed operation. The contribution of this paper is the results of the experimental implementation found of the two types of observers. The results found are perfect, they are similar to the simulation results. The use of this method will solve several problems encountered previously with the sensors.

## REFERENCES:

- [1] Kojabadi H.M., Ghribi M., "MRAS-based adaptive speed estimator in PMSM drives". Advanced Motion Control AMC'06, 9th IEEE International Workshop, pp. 569 – 572, - Istanbul, Turkey, 2006.
- [2] Hadj Said S., Mimouni F., M'sahli F., Farza M., "High gain observer based on line rotor and stator resistances estimation for IMs", IEEE International Conference on Control Applications Part of 2010 IEEE Multi-Conference on Systems and Control Yokohama, Japan, September 8-10, 2010.
- [3] Monmasson E., Cristea M., "FPGA Design Methodology for Industrial control systems- A Review IEEE trans. Ind. Electron., Vol.54 N°4, pp.1824-1842, August 2007.
- [4] Charaabi L., Monmasson E., and Belkhdja I., "Presentation of an efficient design methodology for FPGA implementation of control system application to the design of an antiwindup PI controller", In Proceedings IEEE IECON, 2002, pp. 1942–1947.
- [5] Bossoufi B., Karim M., Ionita S., Largaoui A., "Indirect Sliding Mode Control of a Permanent Magnet Synchronous Machine: FPGA-Based Implementation with Matlab & Simulink Simulation" Journal of Theoretical and Applied Information Technology (JATIT), pp. 32-42, Vol.29 N°1, 15th July 2011
- [6] Xilinx System Generator for DSP, User guide, UG640(v13.1), march 2011.
- [7] Trabelsi R., Khedher A., Mimouni M.F., M'sahli F., "Backstepping control for an induction motor using an adaptive sliding rotor-flux observer", Electric Power System Research, Elsevier, 2012.
- [8] Xiao X., Li Y., Zhang M., Liang Y., "A sensorless control based on MRAS method in interior permanent-magnet machine drive". Power Electronics and Drives Systems, Peds 2005. International Conference on Vol.1, 16-18 January 2006 pp. 734 – 738.
- [9] Dunningan M.W., Wade S., Williams B.W. Yu X., 'Position control of vector controlled induction machine using Slotine's sliding mode control approach', IEEE Proceedings on Electrical Power Applications, on Industrial Electronics, Vol.145, Issue 3, pp. 231-238, 1998
- [10] Gdaim S., Mtibaa A., Mimouni M.F., "Experimental implementation of Direct Torque Control of induction machine on FPGA". International Review of Electrical

Engineering, Vol.8, N°1, ISSN 1827-666,  
Février 2013.

- [11] Charaabi L., Monmasson E., and Belkhodja I., "Presentation of an efficient design methodology for FPGA implementation of control system application to the design of an antiwindup PI controller", In Proceedings IEEE IECON, 2002, pp. 1942–1947.
- [12] Rajendran R., Devarjan N., "Simulation and implementation of a high performance torque control scheme of IM utilizing FPGA"., International Journal of Computer and Electrical Engineering (IJECE), Vol.2, N°3, ISSN 2088-8708, pp. 277-284, June 2012.
- [13] Rajendran R., Devarjan N., "FPGA based implementation of space vector modulated Direct Torque Control for induction motor drive". International Journal of Computer and Electrical Engineering, Vol.2, N°3, ISSN 1793-8163, June 2010.